Optimized Biorecognition of Cytochrome *c* 551 and Azurin Immobilized on Thiol-Terminated Monolayers Assembled on Au(111) Substrates

B. Bonanni,*,†,‡ A. R. Bizzarri,† and S. Cannistraro†

Biophysics and Nanoscience Centre, CNISM, and CNR-INFM, Dipartimento di Scienze Ambientali, Università della Tuscia, Largo dell'Università, I-01100 Viterbo, Italy

Received: February 17, 2006; In Final Form: April 19, 2006

Molecular recognition between two redox partners, azurin and cytochrome *c* 551, is studied at the single-molecule level by means of atomic force spectroscopy, after optimizing azurin adsorption on gold via sulfhydryl-terminated alkanethiol spacers. Our experiments provide evidence of specific interaction between the two partners, thereby demonstrating that azurin preserves biorecognition capability when assembled on gold via these spacers. Additionally, the measured single-molecule kinetic reaction rate results are consistent with a likely transient nature of the complex. Interestingly, the immobilization strategy adopted here, which was previously demonstrated to favor electrical coupling between azurin (AZ) and the metal electrode, is also found to facilitate AZ interaction with the redox partner, if compared to the case of AZ directly adsorbed on bare gold. Our findings confirm the key role of a well-designed immobilization strategy, capable of optimizing both biorecognition capabilities and electrical coupling with the conductive substrate at the single-molecule level, as a starting point for advanced applications of redox proteins for ultrasensitive biosensing.

Introduction

Recent years have witnessed significant interest in the development of ultrasensitive, fast, and reliable biosensors, commonly based on biomolecules coupled to microelectronic or optical transducers and on a variety of surface-based detection principles. The detection relies on biorecognition between the reagent biomolecules and sample molecules: when the biomolecules selectively react with (bind to) the molecules they are designed to detect, a clear signal is obtained from the sensor. In recent times important advances in biotechnology and nanotechnology have taken place, opening a way to the development of single-biomolecule-based nanobiosensors. Most modern biosensors are capable of detecting very low amounts of various biological species (in the range of 10^{-18} M) such as cells, proteins, viruses, and bacteria,[1,2] and the sensitivity is currently improving down to the limit of single-molecule detection.[3,4]

With reference to such applications, planar gold surfaces emerged as attractive solid supports for biomolecules, thanks to their ability to enable both optical and electrical transduction schemes,[1,5] as well as to the possibility to stably bind various kinds of proteins.[6] In this connection, much work has been dedicated to the controlled adsorption of metalloproteins on gold: these biomolecules have important characteristics, such as electron transfer (ET) properties and the possibility of gating redox activity, with promising applications in the integration with submicrometer-sized electronic components.[7,8]

An efficient electrical communication between the biomolecule and the electrode is desirable and can be achieved by covalent linking the protein to the metal surface. For direct chemisorption of ET proteins on Au substrates, the high affinity of protein disulfides and thiols for gold have been often exploited, as for instance for azurin (AZ) from *Pseudomonas aeruginosa*,[9−11] which bears an exposed disulfide moiety (Cys3-Cys26), located opposite to the copper active site, suitable for covalent linking to gold.[12]

Noticeably, the preserved biorecognition capability of the single adsorbed biomolecule is a fundamental requirement for the application of redox proteins to nanobiosensors. In this respect, integration of the ET protein with a conductive support—which serves as a transducer—offers additional detection modes of individual recognition events (e.g., by revealing very small variations in the conductive response).

In general, molecular interaction between two physiological partners may be investigated at the single-molecule level by atomic force spectroscopy (AFS). As a matter of fact, by this technique, unbinding forces of individual ligand−receptor pairs can be probed by recording force versus distance cycles on a surface-bound ligand by means of an atomic force microscopy (AFM) tip functionalized with the receptor.[13] Interestingly, AFM can be also employed as an ultrasensitive detection tool for revealing biorecognition.[14] For instance, arrays of AFM cantilevers suitably functionalized with biomolecules capable to bind their physiological partners are recently being exploited in bioanalytics.[15]

Recently, AFS experiments performed by our group demonstrated, for the first time for two redox partners, that biorecognition capability was preserved after directly linking one of the partners to a conductive substrate.[16] More specifically, AZ from *P. aeruginosa* was first chemisorbed on bare gold; after verifying that functionality and ET capabilities of the adsorbed molecules were preserved,[11,17] the interaction with the redox partner cytochrome *c* 551 (C551) was investigated, at the single-molecule level, by AFS. Such interaction is believed to occur through different steps:[18] after protein recognition and specific binding, ET between the two partners can take place with optimal efficiency; the complex subsequently dissociates to yield

* Corresponding author. Phone: +39 0761 357027. Fax: +39 0761 357179. E-mail: bonanni@unitus.it.

† CNISM.

‡ CNR-INFM.

10.1021/jp0610315 CCC: $33.50
Published on Web 07/08/2006

the products. Our AFS experiments provided a clear evidence of specific recognition events between the two partners.[16] However, despite the experimental indication of AZ functionality retention upon gold adsorption, a significant percentage of the immobilized proteins were found to display a reduced height over the gold substrate so that (partial) denaturation could not be completely ruled out.[17,19,20] As a matter of fact, the direct chemisorption of the protein to the electrode may lead to a strong protein−metal interaction which, in some cases, can result in protein denaturation.[21] Alternative immobilization strategies of metalloproteins on gold have been proposed.[22−26] For instance, thiol-terminated chains can be easily deposited on Au surfaces via S−Au bonds[27,28] forming self-assembled monolayers (SAMs); the reactive function at the other end of the spacer can be suitably chosen for specific interaction with one group of the protein.

Recently, we proposed an immobilization strategy for AZ on gold[29] consisting of sulfhydryl-terminated spacers capable of binding gold at one end and reacting with thiol groups of the biomolecule at the other end,[30] thus leading to a stable and well-defined protein adsorption. Such an immobilization strategy, if compared to adsorption on a bare Au surface, reduces protein−metal interactions (with consequent recovered height of the AZ molecules over the substrate) and facilitates the tunneling current through the protein.[29] For this reason, such an assembling approach is proposed as an effective way for integrating redox metalloproteins with a gold electrode. The preserved AZ biorecognition capability upon this immobilization strategy is, however, still an open question and will be addressed in the present paper.

More specifically, here we investigate the effectiveness of molecular recognition between AZ and its redox partner C551, after optimizing AZ immobilization on gold via the introduction of the sulfhydryl-terminated SAMs. With such an immobilization strategy the AZ molecules are linked to the spacer (and then to gold) via Cys3 and Cys26 residues so that the proteins are in a configuration in which the hydrophobic patch, involved in the interaction with C551,[31,32] is oriented up[12]—away from the electrode surface—for optimal interaction with C551.

The study has been performed at the level of a single molecule by means of AFS, namely, by recording force versus distance cycles on the AZ/SAM/gold sample by using a C551-functionalized tip. The present study represents a novelty since, to the best of our knowledge, only one paper has been published concerning AFS on redox partners.[16] The results are also discussed in connection with analogous experiments on bare gold-immobilized AZ.

Experimental Methods

AZ and C551 from *P. aeruginosa* and all chemicals were purchased from Sigma Aldrich (St. Louis, MO). AZ was diluted in 50 mM sodium phosphate buffer solution, pH 7, at a final concentration of 15 μM. The C551 solution was passed through a Sephadex G-25 desalting column (PD10, Pharmacia, Peapack, NJ) to change the initial ammonium acetate pH 4.7 buffer to 50 mM sodium phosphate buffer solution, pH 7.

The substrates (from Arrandee) consist of vacuum-evaporated thin gold films (thickness 250 nm) on borosilicate glass. The Au−glass substrates were flame-annealed, to obtain atomically flat Au(111) terraces over hundreds of nanometers, as confirmed by contact mode AFM characterization, with a typical roughness of about 0.1−0.05 nm.

For gold functionalization with SAM of sulfhydryl-terminated alkanethiols, the annealed substrates were first immersed in an ethanolic solution of 1 mM mercaptoethanolamine for 24 h at room temperature. The samples, now exposing amine groups, were immersed for 2 h at room temperature in a solution of 20 mM *N*-succinimidyl-*S*-acetylthiopropionate (SATP), dissolved in 10% dimethyl sulfoxide (DMSO) and 90% PBS buffer solution, pH 7. Subsequently, the sulfhydryl groups of the spacers were deprotected by exposing the sample to a solution of 0.5 M hydroxylamine in 50 mM PBS, pH7, 25 mM ethylenediamine tetraacetic acid (EDTA), and 50 mM dithiothreitol (DTT) for 20 min. For details of chemical reactions, see ref 29. Samples were then rinsed with Milli-Q water. AFM and scanning tunneling microscopy (STM) imaging of the modified gold confirmed that a homogeneous coverage of the Au(111) surface was attained, consistent with the assembling of a sulfhydryl-terminated alkanethiol monolayer, in agreement with data from the literature.[30,33] The samples were then incubated at 4 °C with 15 μM AZ solution, for times ranging between several minutes and few hours in order to adjust surface coverage from submonolayer (for AZ single-molecule characterization) to almost full coverage. To remove any unadsorbed material, samples were gently rinsed with buffer solution and immersed in the fluid cell containing buffer for immediate fluid imaging and force spectroscopy. A schematic representation of the final AZ/SAM/gold sample is shown in Figure 1a.

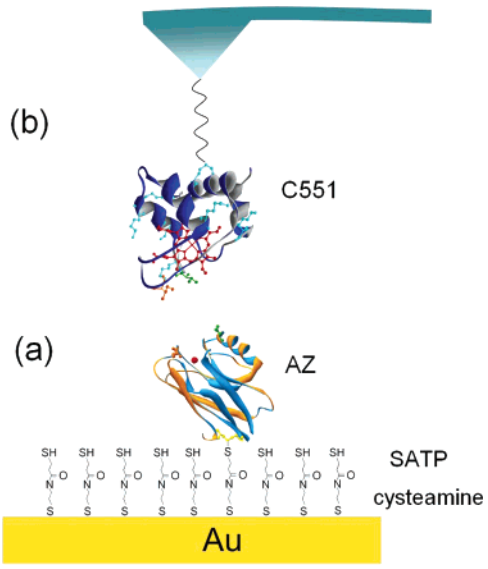

Figure 1. (a) Immobilization of AZ molecules to a gold surface via the introduction of sulfhydryl-terminated SAM. The linkage of the SAM to the gold occurs through S−Au bonds, whereas the protein is bound to the spacer via S−S− bonds involving protein cysteine residues Cys3 and Cys26, represented in the figure with yellow balls and sticks. (b) Schematic representation of C551 covalently linked to the AFM tip via a heterobifunctional PEG cross-linker which is able to bind one of the eight lysine residues (light blue) of the protein.

C551 was covalently coupled to the tip via a long flexible spacer molecule: by this linkage method, the protein on tip is free to move and reorient over the AZ sample, thus facilitating mutual interaction. The cross-linker used is a heterobifunctional poly(ethylene glycol) (PEG) derivative, already used for experiments on AZ immobilized on a bare gold surface.[16] This linker is 10 nm long and bears an aldehyde (ALD) moiety at one end and *n*-hydroxysuccinimide (NHS) at the other end. The Si_3N_4 cantilevers (Veeco Instruments, Santa Barbara, CA) have been first rinsed in three changes of chloroform and then incubated overnight with ethanolamine−HCl dissolved in DMSO. Subsequent incubation of the tips with PEG solution results in stable binding of the cross-linker NHS end with the amino-treated tip

surface. PEG solution has been adjusted to ensure low density of cross-linkers on the Si_3N_4 surface and therefore single-molecule detection by the tip. Tips functionalized with the PEG were finally immersed in the C551 solution. The cytochrome molecules stably bind to the ALD end of the flexible PEG via one of their eight lysine residues, homogeneously distributed on the molecule's surface. In Figure 1b a schematic representation of the C551−PEG AFM tip is shown. The functionalized tips were stored in buffer solution at 4 °C until use.

The cantilever spring constant of the functionalized tips (nominal value 0.030 N/m) was experimentally determined by thermal noise analysis[34] with an uncertainty of 10% on each cantilever. Measured values for used cantilevers ranged from 0.022 to 0.040 N/m.

Topographic images of the sample surface were taken by using a Nanoscope IIIa/Multimode scanning probe microscope (Digital Instruments) equipped with a 12 μm scanner. The nanoscope was used in contact mode configuration for Au(111) characterization in air. The modified gold surface (with the sulfhydryl-terminated spacers only and also with the adsorbed proteins) was characterized in PBS buffer solution with the AFM operating in tapping mode (TM). The amplitude set point was selected to be 85% of the free amplitude value. For imaging, oxide-sharpened silicon nitride probes (Digital Instruments), 100 or 200 μm long, with nominal spring constants of 0.15 and 0.57 N/m and typical correspondent resonant frequencies of 8−30 kHz, respectively, were used.

Force spectroscopy experiments were performed with the same instrument used for imaging. In this modality, force−distance cycles were recorded over the AZ sample in buffer solution, by using the PEG−C551-functionalized tip. To avoid possible damage of the modified probe, no images were taken with such tips. The maximum force applied to the AZ sample was limited by setting a constant relative trigger of 15−30 nm. Approach and pulling velocities, identical in all force−distance cycles, were in the range of 300−5000 nm/s, whereas the encounter time, namely, the interval between approach and retraction, was set equal to zero.

Results and Discussion

Prior to force spectroscopy experiments, the morphology of AZ single molecules assembled on the modified gold substrate was characterized by TMAFM in buffer solution. A typical AFM image of the AZ/SAM/Au sample used for unbinding force measurements is shown in Figure 2. Single metalloproteins with a globular shape can be clearly discerned over the SAM-modified gold surface, which displays an average roughness of about 0.50 ± 0.04 nm. The imaged metalloproteins do not display mobility or formation of aggregates on the SAM-modified gold, as already observed for AZ chemisorbed on bare gold,[17,19] which is indicative of robust anchoring to the substrate, as expected for covalent immobilization. The protein height on the modified gold has been estimated by cross-sectional analysis. A typical cross-sectional profile over individual AZ molecules, also showing the SAM/Au background, is represented in Figure 2. We found a single-mode distribution of the measured vertical size, with an AZ mean height of 3.4 nm and a standard deviation of 0.8 nm.[29] This value is in good agreement with the 3.1 nm vertical size as estimated from X-ray crystallography data[12] for topological arrangement of the protein on gold with the two cysteine residues oriented toward SAM-modified gold (see Figure 1a). This result differs from what was observed for AZ on bare gold.[17,19] Indeed, when the proteins were directly immobilized on the gold substrate, the mean height was found

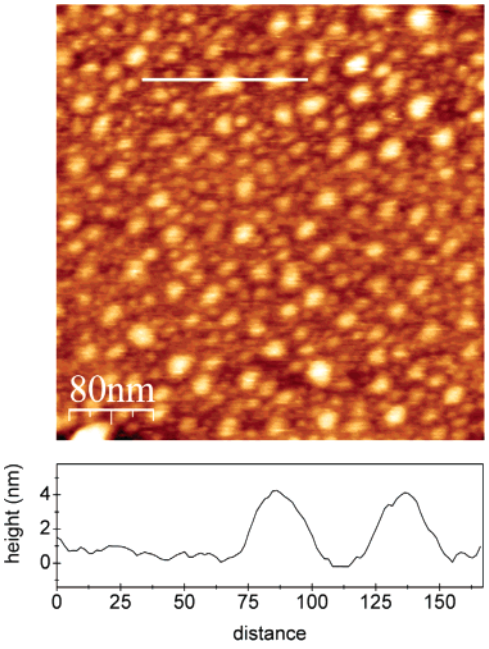

Figure 2. Typical TMAFM image of the AZ/SAM/Au sample used for unbinding force measurements, recorded in buffer solution. A representative cross-sectional profile (recorded along the white line in the image) over individual AZ molecules and the SAM/Au background is also represented.

to be 1.7 nm with a standard deviation of 0.6 nm, namely, significantly lower than what was expected from crystallographic data. In that case a partial denaturation involving a significant population of adsorbed molecules could not be ruled out.[20] Remarkably, the recovered height of AZ over the modified substrate can be reasonably ascribed to nondenaturing adsorption of the molecules on coated gold. As a matter of fact, a reduced protein−metal interaction is expected when a spacer is introduced between gold and the biomolecule, as for the SAM-modified substrate.[28,35,36] Interestingly, STM experiments—previously performed on such samples by our group[29]—have revealed an increased STM contrast of AZ molecules on the sulfhydryl-terminated gold, if compared to the same proteins directly adsorbed on bare Au. The significant (4-fold) increment in the measured STM height for AZ on modified gold testifies to a more efficient electron tunneling between the tip and the substrate, likely due to improved electrical coupling of AZ and substrate, when immobilization is achieved by the cysteamine−SATP linker.[29]

The sulfhydryl-terminated alkanethiol spacer puts AZ in a configuration in which the hydrophobic patch, involved an interaction with C551,[31,32] is oriented up—away from the electrode surface—i.e., facing the tip of an AFM. As a result, this immobilization strategy, coming out as ideal for adsorption of functional AZ on gold with good electrical coupling between protein and substrate, represents an optimal starting point for the study of specific interactions between gold-immobilized AZ and its redox partner C551. To this aim, the imaging tip was replaced with the C551-functionalized tip and force spectroscopy experiments were performed on the AZ sample. A typical AFM force−distance cycle, recorded at a scan rate of 2790 nm/s, is shown in Figure 3.

The hysteresis between the approach and retraction traces is indicative of AZ−C551 interaction. More specifically, the retrace curve displays the characteristic nonlinear behavior of PEG linker stretching (schematically shown in the inset) in accordance with the wormlike chain polymer−elasticity model;[37]

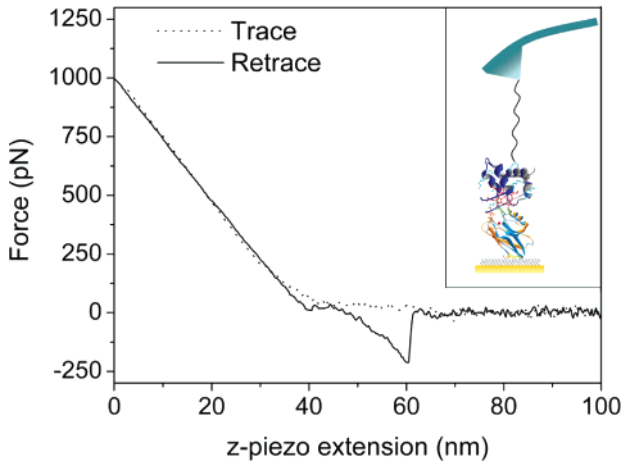

Figure 3. Characteristic force vs distance cycle recorded with a C551-functionalized AFM tip over an AZ/SAM/Au sample showing a rupture event during retraction. Inset: schematic representation of tip retraction after recognition and binding of the proteins, with typical stretching of the PEG cross-linker.

subsequent AZ−C551 unbinding is detectable as a pull-off jump. In other words, the typical PEG stretching serves as a criterion to discriminate real single unbinding events from unspecific adhesion. The length of the stretched PEG, as estimated by measuring the distance between the contact point and the pull-off jump, is 23 ± 7 nm and meets typical values found in force spectroscopy experiments performed with similar PEG cross-linkers.[16,38] This result is consistent with the fact that the selected pull-off jumps correspond to PEG stretching and following protein unbinding whereas a possible unfolding of one of the interacting proteins is unlikely.[39]

Similar curves, as that shown in Figure 3, were recorded over different sites on the sample surface, corresponding to an unbinding probability in the range 8.9% ± 0.7%; only a very few adhesion events (characterized by linear retrace force slope) were observed. Such an unbinding probability is lower than the 18% value found for full covered AZ/Au samples[16] and is likely to be ascribed to the submonolayer coverage of the samples examined. Indeed, the typical coverage of the SAM/Au substrate with AZ molecules, as estimated from AFM imaging (see also Figure 2), was in the range of 1100−1200 particles/μm^2, whereas the molecule density for the AZ/Au samples previously investigated[16] was estimated by AFM to be about 2100 particles/μm^2, namely, 60% higher. Such a difference is consistent with a reduction of about 50% of detected unbinding events for the AZ/SAM/Au samples studied here.

As a control experiment for validating the specificity of the AZ−C551 interaction, free AZ (30 μM) was added to the PBS solution in the AFM fluid cell, as a competing ligand for C551 on the tip ("tip blocking"). As a consequence, the unbinding probability was significantly reduced, changing from a mean value of 8.9% ± 0.7% to 3.3% ± 0.2%, therefore decreasing by about 63%. The persistence of a 3% residual unbinding activity, observed in many blocking experiments even in very effective blocking conditions, has often been related to the forced interaction between the two molecules, due to the experimental setup.[16,40,41] The tip was then washed in copious PBS buffer, and the AZ solution in the fluid cell was replaced by fresh PBS solution. In this way, the system could be reactivated to its full former binding functionality, the final unbinding probability being 8.7% ± 0.4%, namely, comparable to the initial one.

From the pull-off jump of the retraction curves the unbinding forces were measured. Values below the noise level, namely, the standard deviation of the flat portion of the force−distance curve, were not taken into account. The unbinding force histograms in the three experimental conditions described above are shown in Figure 4a−c. Apart from a significant change in the total (integrated) unbinding probability, the force distributions before tip blocking (Figure 4a), during blocking (Figure 4b), and after washing (Figure 4c) look very similar, displaying essentially a single mode at about 180 pN. The similarity of the distributions in the three experimental conditions is a further indication that a specific interaction, which can be fully reactivated after washing, is monitored.

To further validate the specificity of the detected unbinding events, force−distance cycles have been recorded over the very same AZ/SAM/Au sample by means of a bare tip. In this case, all "unbinding events" show a linear dependence of force versus distance, which is typical of adhesion. Moreover, the measured mean length scale of the detected pull-off jumps is 7 ± 2 nm; such a value is much lower than the typical length scale of unbinding events recorded with the PEG−C551-functionalized tip (23 ± 7 nm, as expected for PEG stretching and following C551−AZ unbinding), whereas it is consistent with the typical length scale of nonspecific adhesion.[39] Importantly, the force distribution of the pull-off events detected with the bare tip (see Figure 4d−f), being centered at 105−115 pN, is very unlike that from the analogous distribution obtained with the C551-functionalized tip (see Figure 4a−c), as for different interactions detected with the two tips. Additionally, conversely to what was observed with the C551-functionalized tip, the blocking agent has no effect on the number of pull-off events detected by the bare tip, consistent with the nonspecificity of the detected interaction: the "unbinding" probability remains constant at about 3.5% both in buffer solution (Figure 4, parts d and f) and in the presence of the blocking agent (Figure 4e).

Concerning the absolute value of the most probable AZ−C551 unbinding force, we have to bear in mind that it usually depends on the loading rate that is exerted on the bound complex, i.e., on the time dependency of external forces.[42−44] Therefore, a comparison with other complexes may be performed only if referring to data recorded in the same experimental conditions (i.e., the same loading rate). The loading rate is calculated by taking into account the PEG spacer elasticity, specifically by multiplying the AFM retract velocity by the cantilever−PEG effective spring constant, the latter being estimated from the linear part of the retraction curve preceding the pull-off jump.[45] By varying the scan velocity in the range of 300−4200 nm/s, several loading rates in the range of 10^3 to 10^5 pN/s were explored. To get the statistical distributions of the unbinding forces, 1000 force−distance cycles were recorded at each loading rate. In Figure 5 the force distributions corresponding to the minimum and maximum loading rate sampled are shown. We observe a more than 2-fold increase of the measured unbinding forces, the most probable values (obtained by fitting the histograms to a Gaussian function) changing from 114 ± 15 pN to 267 ± 10 pN.

At intermediate values of the loading rate we observe a continuous upward shift of the rupture forces, consistent with the dynamic response of other ligand−receptor pairs.[45−48] Figure 6 summarizes the dynamic response of AZ−C551 pairs to all the loading rates examined. In this range, we observe that the most probable unbinding force (determined by fitting a Gauss distribution to the histogram data) progressively increases with almost a linear trend versus the logarithm of the loading rate.

This result suggests that our data can be examined in the context of Bell's model,[42] which accounts for complex dis-

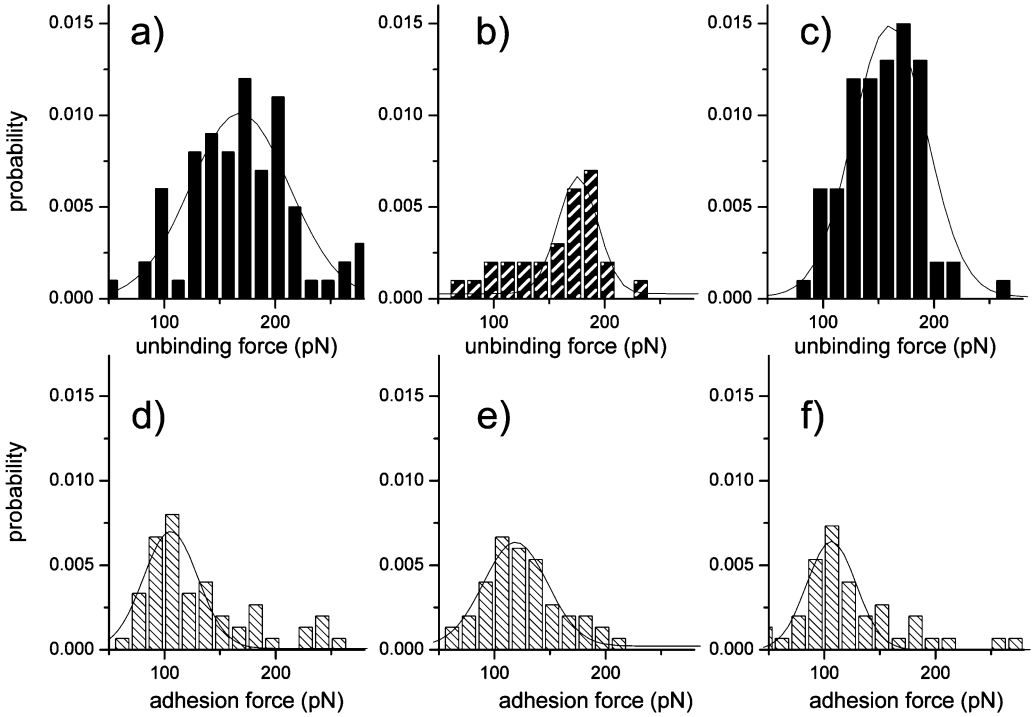

Figure 4. Upper panel: statistical distributions of unbinding forces recorded over the AZ/SAM/Au sample with a C551-functionalized tip in different experimental conditions before (a) and during (b) tip blocking and (c) after tip washing. Lower panel: same as in the upper panel but with a bare tip in three different experimental conditions, namely, before (d) and during (e) tip blocking and (f) after tip washing. Gaussian fits to the histograms are also shown.

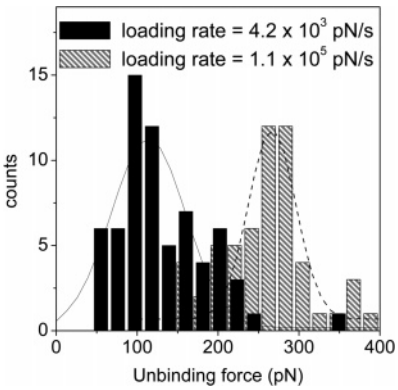

Figure 5. Statistical distribution of the unbinding force for maximum and minimum values of the applied loading rate. The most probable unbinding force is derived as the center of the Gaussian which best fits the histograms.

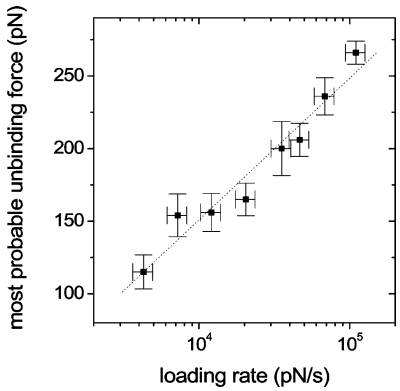

Figure 6. Most probable unbinding forces plotted logarithmically against the corresponding loading rates. Force values result from a Gaussian fit to the histogram distribution, as shown in Figure 4 for minimum and maximum loading rate. Force statistical errors are calculated as $2\sigma/N^{1/2}$ (where σ is the Gaussian standard deviation and N the number of events) corresponding to a 95.4% confidence level, whereas errors on loading rates are evaluated from uncertainty in the effective spring constant of the cantilevers. The dotted line is a numerical fit of experimental data to the Bell model, as described in the text. Best fitting parameters are $k^0_{off} = 6.7 \pm 2.3\ s^{-1}$ and $x_\beta = 0.098 \pm 0.009$ nm.

sociation in the presence of a single energy barrier in the thermally activated regime. According to Bell, the dissociation rate k_{off} of a bond is amplified by the application of an external force f as follows, $k_{off}(f) = k^0_{off} \exp[fx_\beta/(k_BT)]$, where k^0_{off} is the dissociation rate in the absence of the applied force, k_B is the Boltzmann's constant, and x_β is a parameter related to the length scale of the interaction. If the load on the complex increases with a constant rate ν (as in our force spectroscopy measurements), the most probable unbinding force depends logarithmically on the loading rate according to the following relation: $F^* = (k_BT/x_\beta) \ln[(\nu x_\beta)/(k_BTk^0_{off})]$. Therefore, by fitting our data with the previous relation, interesting thermodynamical information concerning the AZ−C551 complex can be derived.[44] As a matter of fact, we can determine the thermal dissociation rate k^0_{off} in the absence of applied force, whereas the second fitting parameter, x_β, corresponds to the width of the potential barrier between the bound complex and the transition state.[44] The best fit to our data, plotted in Figure 6 as a dotted line, provides an estimate for x_β which is found to be 0.098 ± 0.009 nm, whereas for the off-rate we get $k^0_{off} = 6.7 \pm 2.3\ s^{-1}$. Such a value is significantly higher than off-rates typical of "stable" complexes and is indicative of a quite fast complex dissociation, consistent with the transient nature of ET complexes.[18,49] Indeed, AFS experiments have provided off-rate values in the range of 10^{-3} to $10^{-2}\ s^{-1}$ for many antigen−antibody pairs[46,50,51] or protein/DNA interactions[52] as well as for complementary DNA strands;[53,54] the estimated value for the well-known high-affinity complex biotin−avidin is even lower, $10^{-5}\ s^{-1}$, as from ref 45.

It is worth comparing the loading rate dependence of the AZ−C551 system just discussed, referring to AZ immobilized on

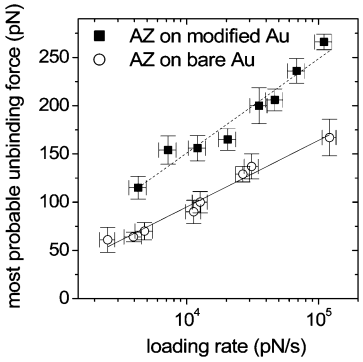

Figure 7. Loading rate dependence of the most probable unbinding forces, as evaluated from the Gaussian fit to the histogram distributions, for AZ−C551 when AZ is immobilized either on modified Au (filled squares) or bare Au (open circles). Lines correspond to the numerical fit of the experimental data to the Bell model. Statistical errors on force values are given by $2\sigma/N^{1/2}$ (with σ being the Gaussian standard deviation and N the number of events) for a confidence level of 95.4%, whereas errors on loading rates are evaluated from uncertainty in the effective spring constant of the cantilevers.

modified gold (AZ/SAM/Au), with analogous data for AZ−C551 when AZ is immobilized on bare gold (AZ/Au).[16] For the sake of clarity, data from the two experiments are reported in the same plot in Figure 7. At first glance we notice that the AZ−C551 rupture forces in the case of AZ/Au are lower that those measured for AZ/SAM/Au. For loading rates in the range of 4×10^3 pN/s and 10^5 pN/s, the most probable AZ−C551 unbinding force increases from 65 to 165 pN for AZ/Au, whereas it goes from 114 to 267 pN for Az/SAM/Au. More importantly, the thermal off-rate, k^0_{off}, when AZ is directly immobilized on bare gold, is 14 ± 2 s^{-1}, about twice the value estimated when AZ is immobilized on the modified gold. This finding indicates that AZ molecules immobilized on gold via the SAM fit more tightly to C551, as also suggested by the higher measured rupture forces. In other words, AZ interaction with its redox partner seems to be accompanied by a rise in binding affinity when immobilization on gold is accomplished via a linker. Indeed, the introduction of a spacer, besides reducing the protein−metal interaction preserving molecular functionality, is likely to leave the protein free to move and reorient for optimal interaction with its counterpart. Concerning the value of x_β, related to the potential barrier width between the complex bound and transition state,[44] we observe only a slight decrease of the estimated value for AZ/SAM/Au if compared to that of AZ/Au. In general, a relatively small potential barrier width reflects the resistance of the macromolecules against bond rupture.[55] In this case, the slightly lower value of x_β for AZ−C551 when AZ is immobilized on gold via the spacer is consistent with the higher rupture forces measured, as well as with the lower off-rate at zero force. As a result, all our findings consistently suggest that modification of the gold substrate via the sulfhydryl-terminated alkanethiol monolayer provides AZ molecules with a higher flexibility on the substrate which is likely to facilitate AZ−C551 interaction and complex formation. Importantly, such an immobilization strategy (which was found to be ideal for adsorption of functional AZ on gold both for the preserved morphological characteristics and the good electrical coupling with the substrate) represents and optimal starting point for advanced applications of redox proteins in the implementation of ultrasensitive biosensors, possibly based on novel detection modes (e.g., electric) for biorecognition.

Conclusions

The specific individual recognition of the two redox partners AZ and C551 has been investigated here by AFS experiments. The measured single-molecule kinetic reaction rates were found consistent with a likely transient nature of the complex. The immobilization strategy adopted, based on the introduction of a spacer between the AZ molecules and the gold substrate, seems to assemble proteins with a configuration in which complex formation is favored if compared to the case of AZ immobilization on bare gold, as evidenced by significant decrease of the dissociation rate. Consistently, the measured unbinding forces for the AZ−C551 complex are higher if AZ is linked to gold via the spacer with respect to direct adsorption on gold.

Our results confirm that great advantage may be offered by a well-designed immobilization strategy for protein adsorption on metal substrates in view of optimizing single-molecule biorecognition capability, with preserved efficient conduction through the molecule toward the electrode. As a matter of fact, the immobilization strategy we adopted for AZ on gold had been demonstrated to facilitate the tunneling current through the protein and is found here to provide the biomolecule with the needed flexibility for optimization of partner recognition and binding.

In conclusion, a well-designed immobilization strategy is confirmed to be a crucial step in future developments of nanobiosensor systems. In particular, the optimized biorecognition capability in conjunction with a good electrical coupling of the adsorbed protein with the metal electrode, offering the possibility to test different detection modes for optimal biorecognition sensing, deserves challenging perspectives for the implementation of novel artificial biomolecular recognition structures.

Acknowledgment. The authors thank Professor P. Hinterdorfer from Institute for Biophysics, University of Linz, Austria, for kindly providing the heterobifunctional PEG cross-linker. Thanks are due to Francesca Luciani for her preliminary AFS measurements. This work has been partially supported by the FIRB-MIUR Project "Molecular Nanodevices", the PRIN-MIUR 2004 project and the Innesco-CNISM Project 2005.

References and Notes

(1) Nakamura, H.; Karube, I. *Anal. Bioanal. Chem.* **2003**, *377*, 446.
(2) Rosi, N. L.; Mirkin, C. A. *Chem. Rev.* **2005**, *105*, 1547.
(3) Albrecht, C.; Blank, K.; Lalic-Mülthaler, M.; Hirler, S.; Mai, T.; Gilbert, I.; Schiffmann, S.; Bayer, T.; Clausen-Schaumann, H.; Gaub, H. E. *Science* **2003**, *301*, 367.
(4) Ruckstuhl, T.; Enderlein, J.; Jung, S.; Seeger, S. *Anal. Chem.* **2000**, *72*, 2117.
(5) Ghindilis, A. L.; Atansov, P.; Wilkins, M.; Wilkins, E. *Biosens. Bioelectron.* **1998**, *13*, 113.
(6) Willner, I.; Willner, B. *Trends Biotechnol.* **2001**, *19*, 222.
(7) Willner, I.; Katz, E. *Angew. Chem., Int. Ed.* **2000**, *39*, 1180.
(8) Zhang, W.; Li, G. *Anal. Sci.* **2004**, *20*, 603.
(9) Chi, Q.; Zhang, J.; Nielsen, J. U.; Friis, E. P.; Chorkendor, I.; Canters, G. W.; Andersen, J. E. T.; Ulstrup, J. *J. Am. Chem. Soc.* **2000**, *122*, 4047.
(10) Friis, E. P.; Andersen, J. E. T.; Kharkats, Y. I.; Kuznestov, A. M.; Nichols, R. J.; Zhang, J.-D.; Ulstrup, J. *Proc. Natl. Acad. Sci. U.S.A.* **1999**, *96*, 1379.
(11) Andolfi, L.; Bruce, D.; Cannistraro, S.; Canters, G. W.; Davis, J. J.; Hill, H. A. O.; Crozier, J.; Verbeet, M. Ph.; Wrathmell, C. L.; Aster, Y. *J. Electroanal. Chem.* **2004**, *565*, 21.
(12) Nar, H.; Messerschmidt, A.; Huber, R.; van de Kamp, M.; Canters, G. W. *J. Mol. Biol.* **1991**, *218*, 427.
(13) Rief, M.; Grubmüller, H. *Chem. Phys. Chem.* **2002**, *3*, 255.
(14) Lang, H. P.; Hegner, M.; Gerber, C. *Materials Today* **2005**, *8*, 30.
(15) Frederix, P. L. T. M.; Akiyama, T.; Staufer, U.; Gerber, Ch.; Fotiadis, D.; Müller, D. J.; Engel, A. *Curr. Opin. Chem. Biol.* **2003**, *7*, 641.

(16) Bonanni, B.; Kamruzzahan, A. S. M.; Bizzarri, A. R.; Rankl, C.; Gruber, H. J.; Hinterdorfer, P.; Cannistraro, S. *Biophys. J.* **2005**, *89*, 2783.

(17) Bonanni, B.; Alliata, D.; Andolfi, L.; Bizzarri, A. R.; Cannistraro, S. In *Surface Science Research Developments*; Norris, C. P., Ed.; Nova Science Publishers: New York, 2005; p 1.

(18) Crowley, P. B.; Ubbink, M. *Acc. Chem. Res.* **2003**, *36*, 723.

(19) Bizzarri, A. R.; Andolfi, L.; Stchakovsky, M.; Cannistraro, S. *J. Nanotechnol.* **2005**, *1*, a0100.

(20) Davis, J. J.; Hill, H. A. O. *Chem. Commun.* **2002**, 393.

(21) Zhou, Y.; Nagaoka, T.; Zhu, G. *Biophys. Chem.* **1999**, *79*, 55.

(22) Wei, J.; Liu, H.; Dick, A. R.; Yamamoto, H.; He, Y.; Waldeck, D. H. *J. Am. Chem. Soc.* **2002**, *124*, 9591.

(23) Salamon, Z.; Hazzard, J. T.; Tollin, G. *Proc. Natl. Acad. Sci. U.S.A.* **1993**, *90*, 6420.

(24) Sagara, T.; Murumaki, H.; Igarashi, S.; Sato, H.; Niki, K. *Langmuir* **1991**, *7*, 3190.

(25) Cavalleri, O.; Natale, C.; Stroppolo, M. E.; Relini, A.; Cosulich, E.; Thea, S.; Novi, M.; Gliozzi, A. *Phys. Chem. Chem. Phys.* **2000**, *2*, 4630.

(26) Ferretti, S.; Paynter, S.; Russell, D. A.; Sapsford, K. E.; Richardson, D. J. *Trends Anal. Chem.* **2000**, *19*, 530.

(27) Ulman, A. *Chem. Rev.* **1996**, *96*, 1533.

(28) Weisshaar, D. E.; Lamp, B. D.; Porter, M. D. *J. Am. Chem. Soc.* **1992**, *114*, 5860.

(29) Andolfi, L.; Bizzarri, A. R.; Cannistraro, S. *Thin Solid Films* **2006**, in press.

(30) (a) Smith, E. A.; Wanat, M. J.; Cheng, Y.; Barreira, S. V. P.; Frutos, A. G.; Corn, R. M. *Langmuir* **2001**, *17*, 2502. (b) Wegner, G. J.; Lee, H. J.; Marriott, G.; Corn, R. M. *Anal. Chem.* **2003**, *75*, 4740.

(31) Cutruzzolà, F.; Arese, M.; Ranghino, G.; van Pouderoyen, G.; Canters, G.; Brunori, M. *J. Inorg. Biochem.* **2002**, *88*, 353.

(32) Bizzarri, A. R.; Brunori, E.; Bonanni, B.; Cannistraro, S. *Biophys. J.* **2006**, submitted for publication.

(33) (a) Wirde, M.; Gelius, U.; Nyholm, L. *Langmuir* **1999**, *15*, 6370. (b) Yam, C.-M.; Pradier, C.-M.; Salmain, M.; Marcus, P.; Jaouen, G. *J. Colloid Interface Sci.* **2001**, *235*, 183.

(34) Hutter, J. L.; Bechhoefer, J. *Rev. Sci. Instrum.* **1993**, *64*, 1868.

(35) Gaigalas, A. K.; Niaura, G. *J. Colloid Interface Sci.* **1997**, *193*, 60.

(36) Zhang, J.; Christensen, H. E. M.; Ooi, B. L.; Ulstrup, J. *Langmuir* **2004**, *20*, 10200.

(37) Kienberger, F.; Pastushenko, V. P.; Kada, G.; Gruber, H. J.; Riener, C.; Schindler, H.; Hinterdorfer, P. *Single Mol.* **2000**, *1*, 123.

(38) Hinterdorfer, P.; Kienberger, F.; Raab, A.; Gruber, H. J.; Baumgartner, W.; Kada, G.; Riener, C.; Wielert-Badt, S.; Borken, C.; Schindler, H. *Single Mol.* **2000**, *1*, 99.

(39) Ratto, T. V.; Langry, K. C.; Rudd, R. E.; Balhorn, R. L.; Allen, M. J.; McElfresh, M. W. *Biophys. J.* **2004**, *86*, 2430.

(40) Hinterdorfer, P.; Baumgartner, W.; Gruber, H. J.; Schilcher, K.; Schindler, H. *Proc. Natl. Acad. Sci. U.S.A.* **1996**, *93*, 3477.

(41) Wielert-Badt, S.; Hinterdorfer, P.; Gruber, H.; Lin, J. T.; Badt, D.; Wimmer, B.; Schindler, H.; Kinne, R. K.-H. *Biophys. J.* **2002**, *82*, 2767.

(42) Bell, G. I. *Science* **1978**, *200*, 618.

(43) Evans, E.; Ritchie, K. *Biophys. J.* **1997**, *72*, 1541.

(44) Guthold, M.; Superfine, R.; Taylor, R. M., II. *Biomed. Microdevices* **2001**, *3*, 9.

(45) Yuan, C.; Chen, A.; Kolb, P.; Moy, V. T. *Biochemistry* **2000**, *39*, 10219.

(46) Schwesinger, F.; Ros, R.; Strunz, T.; Anselmetti, D.; Guntherodt, H.-J.; Honegger, A.; Jermutus, L.; Tiefenauer, L.; Pluckthun, A. *Proc. Natl. Acad. Sci. U.S.A.* **2000**, *97*, 9972.

(47) Zhang, X.; Bogorin, D. F.; Moy, V. T. *Chem. Phys. Chem.* **2004**, *5*, 175.

(48) Eckel, R.; Ros, R.; Decker, B.; Mattay, J.; Anselmetti, D. *Angew. Chem., Int. Ed.* **2005**, *44*, 484.

(49) Nooren, I. M. A.; Thornton, J. M. *J. Mol. Biol.* **2003**, *325*, 991.

(50) Fritz, J. A.; Katopodis, G.; Kolbinger, F.; Anselmetti, D. *Proc. Natl. Acad. Sci. U.S.A.* **1998**, *95*, 12283.

(51) Kokkoli, E.; Ochsenhirt, S. E.; Tirrell, M. *Langmuir* **2004**, *20*, 2397.

(52) Bartels, F. W.; Baugmarth, B.; Anselmetti, D.; Ros, R.; Becker, A. *J. Struct. Biol.* **2003**, *143*, 145.

(53) Strunz, T.; Oroszlan, K.; Schafer, I.; Güntherodt, H.-J. *Proc. Natl. Acad. Sci. U.S.A.* **1999**, *96*, 11277.

(54) Schumakovitch, I.; Grange, W.; Strunz, T.; Bertoncini, P.; Guntherodt, H. J.; Hegner, M. *Biophys. J.* **2002**, *82*, 517.

(55) Dettmann, W.; Grandbois, M.; André, S.; Benoit, M.; Wehle, A. K.; Kaltner, H.; Gabius, H.-J.; Gaub, H. E. *Arch. Biochem. Biophys.* **2000**, *383*, 157.